https://doi.org/10.2352/ISSN.2470-1173.2018.15.COIMG-132

A Supervised Learning Approach for Dynamic Sampling (SLADS) in Raman Hyperspectral Imaging

Shijie Zhang[a], Zhengtian Song[a], G. M. Dilshan P. Godaliyadda[b], Dong Hye Ye[b], Atanu Sengupta[c], Gregery T. Buzzard[d], Charles A. Bouman[b], and Garth J. Simpson[a]*

[a]Department of Chemistry, Purdue University, West Lafayette, IN, 47907
[b]Department of Electrical and Computer Engineering, Purdue University, West Lafayette, IN, 47907
[c]Dr. Reddy's Laboratory, IPDO, Bachupally Campus, Hyderabad, Telengana-500090, India
[d]Department of Mathematics, Purdue University, West Lafayette, IN, 47907

Correspondence email: gsimpson@purdue.edu

Abstract

A supervised learning approach for dynamic sampling (SLADS) yielded a seven-fold reduction in the number of pixels sampled in hyperspectral Raman microscopy of pharmaceutical materials with negligible loss in image quality (~0.1% error). Following validation with ground-truth samples, sparse sampling strategies were informed in real-time by the preceding set of measurements. In brief, Raman spectra acquired at an initial set of random positions inform the next most information-rich location to subsequently sample within the field of view, which in turn iteratively informs the next locations until a stopping criterion associated with the reconstruction error is met. Calculation times on the order of a few milliseconds were insignificant relative to the timeframe for spectral acquisition at a given sampling location. The SLADS approach has the distinct advantage of being directly compatible with standard Raman instrumentation. Furthermore, SLADS is not limited to Raman imaging, providing a time-savings in image reconstruction whenever the single-pixel measurement time is the limiting factor in image generation.

Background and Motivation

The efficacy of active pharmaceutical ingredients (APIs) can be greatly impacted by their crystalline form. In the specific case of clopidogrel bisulphate, Form I exhibits substantially faster dissolution kinetics and bioavailability than Form II, which is the thermodynamically favored form. As a result, care is taken during the manufacturing process to ensure high yields of the thermodynamically metastable Form I product. Success in these efforts is informed through a suite of measurements, which include Raman spectroscopy. Unfortunately, the limits of detection for bulk ensemble averaged Raman measurements are on the order of ~1%-5%, which is unacceptably high for ensuring long-term stability of the drug product.

Confocal Raman microscopy holds promise for greatly reducing the limits of detection by allowing classification of individual particles with high confidence. For individual Form I or Form II particles, localized Raman from those individual particles corresponds to a local concentration of 100%, enabling classification based on clear differences in the Raman spectra associated with each of the two crystal forms. In this paradigm, in which Raman microscopy allows classification of individual particles, the lower limit of detection is ultimately dictated by the Poisson statistics governing the total number of particles interrogated and the mis-classification rate of the spectroscopic analysis. However, in practice, the measurement time required to perform Raman imaging sets a practical upper bound on the lower limit of detection. Because Raman scattering is a relative weak process, the long integration times required to obtain spectra with sufficient signal to noise greatly limit the broader utility of Raman microscopy for per-particle analysis.

In this context, it is clear that methods capable of enabling Raman imaging with fewer total number of pixels sampled have the potential to correspondingly reduce the time-frame for Raman image acquisition. The faster imaging speeds correspond directly to a reduction in the limits of detection for the same time of analysis. An approach was developed and validated incorporating SLADS in combination with Raman spectral analysis for classification. Initial proof-of-concept studies were performed on Raman images in which complete spectra were obtained at each pixel, followed by implementation of hyperspectral Raman imaging and classification of clopidogrel bisulphate pharmaceutical materials.

Theoretical Foundation

The theoretical foundation of SLADS is detailed in prior work[1]. In brief, for a ground truth underlying object X consisting of N pixels, the set of k measurements at locations S combine to generate the set of known information Y.

$$Y^{(k)} = \begin{bmatrix} s^{(1)}, X_{s^{(1)}} \\ \vdots \\ s^{(k)}, X_{s^{(k)}} \end{bmatrix} \quad (1)$$

The primary goal of the SLADS algorithm is to identify the location $s^{(k+1)}$ that reduces the subsequent reconstruction distortion between the ground truth and recovered images X and $\hat{X}^{(k)}$, respectively. For a binary image, the distortion D is defined by the following.

$$D\left(X_r, \hat{X}_r\right) = \begin{cases} 0 \text{ if } X_r = \hat{X}_r \\ 1 \text{ if } X_r \neq \hat{X}_r \end{cases} \quad (2)$$

Since increasing the number of measurements will generally improve the accuracy of the reconstruction and reduce the distortion, the reduction in distortion R from measurement of the s

pixel after k preceding measurements is given by the following definition.

$$R^{(k;s)} = D\left(X, \hat{X}^{(k)}\right) - D\left(X, \hat{X}^{(k;s)}\right) \quad (3)$$

In practice, X is not known in advance. However, the expected reduction in distortion (ERD = $\bar{R}$) can be estimated from the expectation value of R.

$$\bar{R}^{(k;s)} = E\left[D\left(X, \hat{X}^{(k)}\right) - D\left(X, \hat{X}^{(k;s)}\right) \middle| Y^{(k)} \right] \quad (4)$$

The next best k+1 sampling location corresponds to the position that maximizes the expected reduction in distortion from Eq. 1.4. In SLADS, the relationship between the measurements Y and the ERD is a regression function informed by an offline training process.

$$R^{(s)} \approx \sum_{r \in \Omega} h_r^{(s)} D\left(X_r, \hat{X}_r\right) \quad (5)$$

$$h_r^{(s)} = \exp\left\{ -\frac{c}{2\left(\sigma^{(s)}\right)^2} \|r - s\|^2 \right\} \quad (6)$$

In Eq. 1.6, $\sigma^{(s)} = \min_{t \in S} \left\{ \|s - t\|^2 \right\}$.

Results and Discussion

Initial studies were performed to assess the merits of the SLADS algorithm in hyperspectral image reconstruction. Ground truth spectra were acquired by performing Raman spectroscopy at each pixel in a 128×128 pixel image consisting of a 1:1 mix of Form I and Form II clopidogrel bisulphate particles.

An instrument schematic for the SLADS Raman microscope are shown in **Figure 1**. In brief, random access within the field of view was achieved with a galvanometer mirror pair, followed by Raman spectral acquisition at discrete locations. Spectral classification was performed to determine composition, and that assignment used in the SLADS analysis for selection of the next most judicious sampling location.

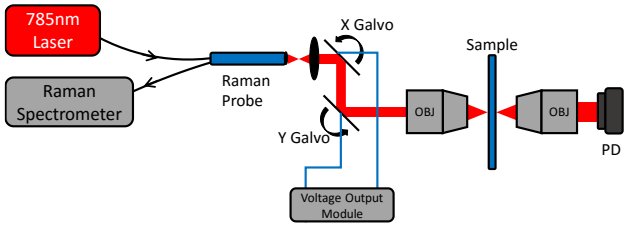

Figure 1. Schematic of the instrument for dynamic sampling image construction for Raman hyperspectral microscopy. A fiber-coupled Raman probe was used to integrate spectroscopy with an existing microscope (Nikon TE2000U). A galvanometer pair was 4f-coupled to the objective using a lens pair (not shown). Following calibration, the galvanometer pair allowed rapid (~1ms) repositioning of the 785 nm Raman laser focal point within the object plane. Concurrent collection of the transmitted 785 nm light allowed for bright field imaging in perfect registry with the Raman imaging.

Comparisons between random sampling and SLADS are shown in **Figure 2** for measurements with a known ground-truth outcome. A mixture of Form I and Form II clopidogrel bisulphate spheroidal particles ~20 µm in diameter were prepared by physical mixing (mortar and pestle), then cast on a transparent glass prior to analysis. Raman spectra were acquired at each location within the field of view and classified as Form I, Form II, or background on a per-pixel basis based solely on the spectroscopy. Classification was performed by spectral dimension reduction through linear discriminant analysis, followed by support vector machine analysis for determination of classification boundaries.

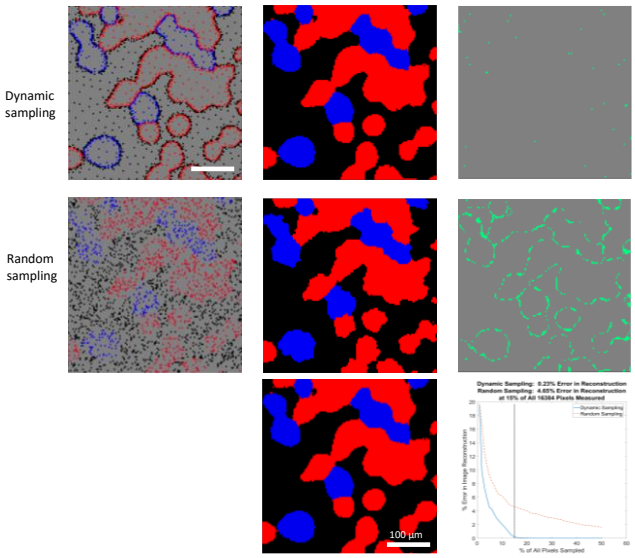

Figure 2. Analysis of SLADS for chemical imaging based on confocal Raman mapping of pharmaceutical materials. Ground truth data were collected by performing Raman sampling at every location in the image (bottom middle) followed by classification at each pixel as Form I (red), Form II (blue), or background (black). Simulations of image reconstructions were then performed for both SLADS and random sampling (top row, and middle row, respectively). Misclassification errors are show in the right-most column for 15% sampling, along with a comparison of the reconstruction errors for both SLADS and random sampling as the fraction of sampled pixels increases.

From inspection of **Figure 2**, dynamic sampling provides clear advantages over random sampling. Most notably, the classification errors corresponding to the border regions between locations of different composition were substantially reduced in SLADS relative to random sampling. From the measured %error based on the ground truth assessment, 15% sampling by SLADS recovered an image with negligible uncertainty relative to the ground truth result, while random sampling of as much as 50% of the pixels still produced measurement errors roughly ten-fold greater.

From these results and other studies incorporating SLADS[1,2], the greatest benefits are likely to be realized in applications in which the measurement time per pixel is necessarily long relative to the combined SLADS calculation time and random access positioning time. In the case of Raman spectroscopy, typical spectral acquisition times greatly exceed the ~1 ms calculation and

random access times. In such scenarios, SLADS has the potential to serve as a general tool for improving image reconstruction quality by efficiently sampling the locations most informative for image reconstruction.

Acknowledgements

The authors gratefully acknowledge financial support from the National Science Foundation GOALI award entitled "Informing Amorphous Formulations Design through Quantitative Nonlinear Optical Analysis", Grant No. 1412888-CHE and from the NIH Grant Number R01GM-103401 from the NIGMS. G.M.D.P.G. and D.H.Y gratefully acknowledges support from Air Force Office of Scientific Research (MURI - Managing the Mosaic of Microstructure, grant # FA9550-12-1-0458) and Air Force Research Laboratory Materials and Manufacturing directorate (contract # FA8650-10-D-5201-0038).

References

1 Godaliyadda, G. M. D. *et al.* A Supervised Learning Approach for Dynamic Sampling. *Electronic Imaging* **2016**, 1-8 (2016).

2 Nicole M. Scarborough *et al.* Synchrotron X-Ray Diffraction Dynamic Sampling for Protein Crystal Centering. *Proc. IS&T Electronic Imaging* **2017** (2017).

Author Biography

The authors represent a multi-disciplinary team with expertise spanning ultrafast optics, image reconstruction algorithm development, and pharmaceutical materials production. The Purdue team spans expertise in Engineering, Mathematics, and Chemistry.

The presenting author Garth J. Simpson received his Ph.D. in Chemistry from the University of Colorado at Boulder in 2000, and started as a faculty member at Purdue University in 2001.He has worked in the area of optics, microscopy, and instrument development for more than 20 years, co-authoring >100 peer reviewed publications and a textbook on the topic.